OPEN

Correspondence and requests for materials should be addressed to J.R.K. (john.r.klein@ uth.tmc.edu)

Hematopoietic not systemic impairment of Roquin expression accounts for intestinal inflammation in Roquin-deficient mice

Dina Montufar-Solis, Nadarajah Vigneswaran, Niyati Nakra, Jeremy S. Schaefer & John R. Klein

Department of Diagnostic and Biomedical Sciences, School of Dentistry, The University of Texas Health Science Center at Houston, Houston, TX 77054 USA.

Roquin, an E3 ligase, is involved in curtailing autoimmune pathology as seen from studies using mice with mutated ($Rc3h1^{san/san}$) or disrupted ($Rc3h1^{gt/gt}$) $Rc3h1$ gene. The extent to which intestinal immunopathology is caused by insufficient Roquin expression in the immune system, or by Roquin impairment in non-hematopoietic cells, has not been determined. Using bone marrow cells from $Rc3h1^{gt/gt}$ mice transferred into irradiated normal mice ($Rc3h1^{gt/gt} \rightarrow$ NL chimeras), we show that inflammation developed in the small intestine, kidney, lung, liver, and spleen. Proinflammatory cytokine levels were elevated in lamina propria lymphocytes (LPLs). Inflammation in the liver was accompanied by areas of hepatocyte apoptosis. Lung inflammation consisted of an influx of both T cells and B cells. Small intestinal LPLs had increased numbers of CD44^{hi}, CD62L^{lo}, KLRG1$^+$, ICOS$^+$ short-lived effector cells, indicating an influx of activated T cells. Following oral infection with *L. monocytogenes*, $Rc3h1^{gt/gt} \rightarrow$ NL chimeras had more liver pathology and greater numbers of bacteria in the Peyer's patches than NL $\rightarrow$ NL chimeras. These findings demonstrate that small intestinal inflammation in $Rc3h1^{san/san}$ and $Rc3h1^{gt/gt}$ mice is due to a failure of Roquin expression in the immune system and not to insufficient systemic Roquin expression.

R oquin, an RNA binding RING finger E3 ubiquitin ligase, localizes to cytosolic RNA granules that regulate mRNA stability and translation. E3 ligases, which determine the specificity of protein degradation by associating with a substrate[1], are defined by their catalytic domains: Homologous to E6-AP Carboxyl Terminus (HECT) domain proteins have intrinsic ligase activities, whereas Really Interesting New Gene (RING) domain proteins function as scaffolds in the degradation process[2]. Roquin is coded for by the $Rc3h1$ gene in mice. Sanroque mice ($Rc3h1^{san/san}$), which have an M199R mutation in the Roquin protein, develop extensive chronic inflammation consisting of lymphadenopathy, splenomegaly, thrombocytopenia, necrotizing hepatitis, increased CD4$^+$ follicular T cells and expression of the inducible costimulator (ICOS) marker of T cell activation[2–6]. Additionally, we recently demonstrated that $Rc3h1^{san/san}$ mice have increased ICOS and OX40 expression in mesenteric lymph node T cells, and that a Crohn's disease-like chronic small intestinal inflammatory response develops in those animals[7]. The latter is of particular interest given the paucity of animal models of small intestine inflammation.

Studies using $Rc3h1$ knockout mice reported that animals had a caudal spine deformity and most animals died within six hours of birth, apparently due to a defect in lung development[8]. Conditional knockouts targeting $Rc3h1$ in T cells or in the entire hematopoietic system failed to exhibit a breach in self-tolerance or changes in follicular T cell differentiation despite an increase in ICOS expression, expansion of CD8 effector cells, and the presence of short-lived effector cells (SLECs)[8]. Roquin-deficient mice generated in our laboratory using a gene trap insertion into the $Rc3h1$ gene ($Rc3h1^{gt/gt}$ mice) also had high post-birth mortality; however, surviving animals developed chronic intestinal inflammation similar to that of $Rc3h1^{san/san}$ mice[7].

Because mice with a disrupted $Rc3h1$ gene ($Rc3h1^{gt/gt}$ mice) have physiological changes that extend beyond the immune system, the intestinal inflammatory response and tissue destruction observed in those animals[7] could be caused by non-immunological perturbations, e.g., Roquin-mediated changes in epithelial cell permeability or effects directed at other non-hematopoietic tissues. To address this, we have used bone marrow (BM) radiation chimeras generated by injecting $Rc3h1^{gt/gt}$ BM into irradiated normal (NL) mice ($Rc3h1^{gt/gt} \rightarrow$ NL chimeras) to

determine whether the intestinal inflammation in *Rc3h1*^{gt/gt} mice was due to a disruption of the *Rc3h1* gene in cells of the immune system (in which case inflammation would be evident), or whether it required systemic Roquin impairment (in which case inflammation would be absent). The findings reported here demonstrate that the inflammatory response in *Rc3h1*^{gt/gt} mice is driven by a direct failure of Roquin expression in cells of the immune system. Moreover, they attest to the utility of using *Rc3h1*^{san/san} and *Rc3h1*^{gt/gt} chimeras to dissect the cellular and molecular mechanisms that regulate the inflammatory response in the intestinal mucosa.

Results

Radiation chimeras generated from *Rc3h1*^{gt/gt} BM develop small intestine inflammation and secrete proinflammatory cytokines. Radiation chimeras were generated as described in the Materials and Methods. Mice were studied between 6 and 21 weeks of age. Histopathological analyses of blinded tissue sections were done for the duodenum, jejunum, ileum, cecum, ascending colon, transverse colon, descending colon, liver, kidney, lung, and spleen. The small intestine of *Rc3h1*^{gt/gt} mice and *Rc3h1*^{gt/gt} → NL chimeras exhibited variable degrees of inflammation and villus atrophy depending upon the region (Fig. 1, rows a and b, respectively). Inflammation and tissue injury of the organs were unremarkable in control NL → NL chimeras (Fig. 1, row c). The average small intestine pathology scores are shown in Fig. 1d, which indicated that inflammation was present throughout the duodenum, jejunum, and ileum of *Rc3h1*^{gt/gt} and *Rc3h1*^{gt/gt} → NL chimeras. Similar to our observation using *Rc3h1*^{san/san} mice[7], *Rc3h1*^{gt/gt} → NL chimeras were devoid of inflammation in the colon (data not shown). *Rc3h1*^{gt/gt} → NL chimeras also had significantly more lamina propria lymphocytes (LPLs) than NL → NL mice (Fig. 1e).

To understand the mechanisms that underlie the intestinal inflammatory response in *Rc3h1*^{gt/gt} → NL chimeras, LPLs from *Rc3h1*^{gt/gt} → NL chimeras and NL → NL chimeras were studied for expression of IL-17A, IFNγ, TNFα, and IL-10 synthesis by intracellular staining. *Rc3h1*^{gt/gt} → NL chimeras (Fig. 2b and c) had increased numbers of IL-17A, IFNγ, and TNFα producing cells compared to NL → NL

chimeras (Fig. 2a and c). When broken down according to CD8^{−} and CD8⁺ populations, CD8^{−} cells had more numbers of cells producing proinflammatory cytokines (Fig. 2d). Similar findings were observed for CD8⁺ cells in *Rc3h1*^{gt/gt} → NL chimeras for IFNγ and TNFα, though not for IL-17A (Fig. 2e). IL-10 levels were not elevated regardless of the type of animal (Fig. 2a and b).

LPLs in *Rc3h1*^{gt/gt} mice and *Rc3h1*^{gt/gt} → NL chimeras have increased numbers of KLRG1⁺ SLECs. We previously reported[7] increased numbers of CD44^{hi} CD62L^{lo} KLRG1⁺ SLECs[9] in mesenteric lymph nodes of *Rc3h1*^{san/san} mice. We have extended those studies here by examining the presence of SLECs in the lamina propria of *Rc3h1*^{gt/gt} and *Rc3h1*^{gt/gt} → NL chimeras. LPLs were isolated from NL mice, *Rc3h1*^{gt/gt} mice, *Rc3h1*^{gt/gt} → NL chimeras, and NL → NL chimeras. Cells were stained for expression of CD44, CD62L, and the killer cell lectin-like receptor G1 (KLRG1). LPLs from all four groups of mice were primarily CD44^{hi} CD62L^{lo} cells (Fig. 3a–d, top histogram panel), a characteristic of intestinal leukocytes due to the low expression of CD62L needed to facilitate migration of cells from lymph nodes to the intestine. Of interest was the finding that, compared to NL mice and NL → NL chimeras, *Rc3h1*^{gt/gt} and *Rc3h1*^{gt/gt} → NL chimeras had proportionally more CD44^{hi} CD62L^{lo} KLRG1⁺ SLECs (Fig. 3a–d, lower histogram panel and Fig. 3e), indicating that there was an influx of SLECs into the lamina propria of both *Rc3h1*^{gt/gt} mice and *Rc3h1*^{gt/gt} → NL chimeras.

KLRG1⁺ LPLs are non-proliferating ICOS⁺ cells that are predominantly effector/memory cells. To further characterize the KLRG1⁺ cell population, LPLs were stained for expression of ICOS and Ki67. ICOS expression is increased in *Rc3h1*^{san/san} mice[4,7]; Ki67 is a marker of cell proliferation[10]. The majority of KLRG1⁺ cells in all four groups of mice were ICOS⁺ (Fig. 4a–d, top histogram panel); however, there was an increase in the overall proportion of ICOS⁺ cells in *Rc3h1*^{gt/gt} mice and *Rc3h1*^{gt/gt} → NL chimeras relative to NL mice and NL → NL chimeras (Fig. 4e). Interestingly, KLRG1⁺ LPLs were primarily non-proliferating cells as seen by a lack of Ki67 staining (Fig. 4a–d, lower histogram panel), and there were fewer
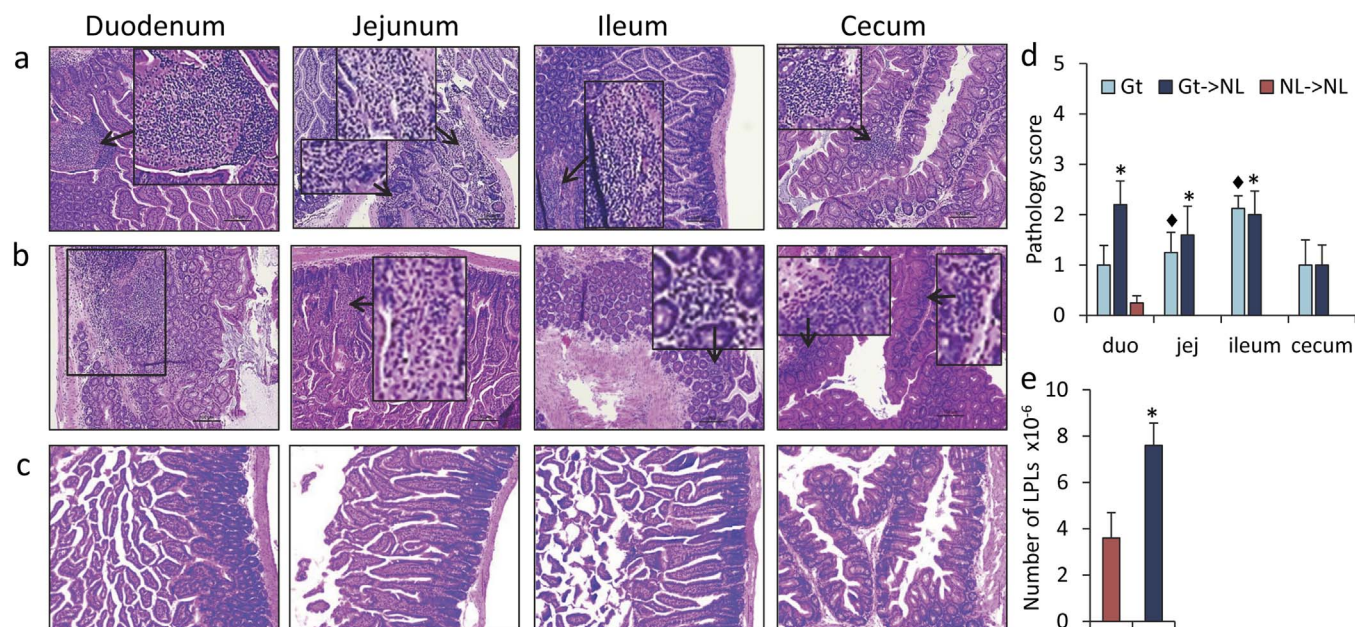

Figure 1 | Histopathological analysis of intestinal tissue sections from (a) *Rc3h1*^{gt/gt} mice, (b) *Rc3h1*^{gt/gt} → NL chimeras, and (c) NL → NL chimeras for the duodenum, jejunum, ileum, and cecum. Note the areas of inflammation (boxed regions) in intestinal tissues of *Rc3h1*^{gt/gt} and *Rc3h1*^{gt/gt} → NL chimeras. Micrographs are 100 × original magnification; scale bars are 100 μm. (d) Mean pathology scores ± SEM of 8 *Rc3h1*^{gt/gt} mice, 5 *Rc3h1*^{gt/gt} → NL chimeras, and 4 NL → NL chimeras. *$p < 0.05$, ◆$p < 0.01$ compared to NL → NL chimeras. (e) Mean numbers of small intestine LPLs ± SEM of 5 *Rc3h1*^{gt/gt} → NL chimeras and 4 NL → NL chimeras. *$p < 0.05$ compared to NL → NL chimeras.
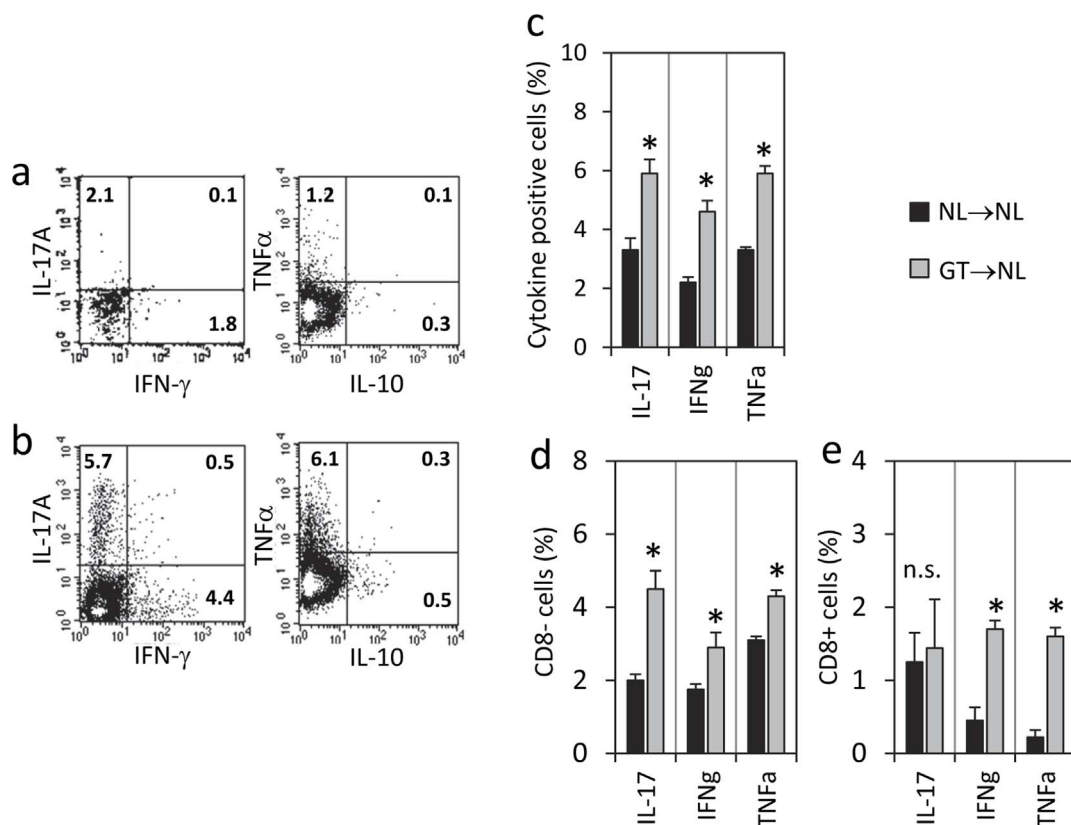
Figure 2 | The proinflammatory cytokines, IL-17A, IFNγ, and TNFα, are produced at higher levels in LPLs of $Rc3h1^{gt/gt} \rightarrow$ NL chimeras compared to NL → NL chimeras. Two-color intracellular staining of LPLs from (a) NL → NL chimeras and (b) $Rc3h1^{gt/gt} \rightarrow$ NL chimeras. (c) Percent of LPLs producing IL-17A, IFNγ, and TNFα in NL → NL chimeras vs. $Rc3h1^{gt/gt} \rightarrow$ NL chimeras. Association of cytokine-secreting cells with (d) CD8⁻ LPLs and (e) CD8⁺ LPLs. *$p < 0.05$. Mean values ± SEM of 3–5 mice per group.

proliferating cells overall in $Rc3h1^{gt/gt}$ mice and $Rc3h1^{gt/gt} \rightarrow$ NL chimeras than in normal mice (Fig. 4f). These findings collectively suggest that there is a continual influx of activated SLECs into the lamina propria of $Rc3h1^{gt/gt}$ mice and $Rc3h1^{gt/gt} \rightarrow$ NL chimeras; however, those cells do not undergo appreciable levels of clonal expansion once they have reached the intestinal mucosa. This is consistent with the observation that KLRG1⁺ cells experience a wave of proliferation during the inductive phase of activation but are generally proliferation non-responsive once they have entered the effector phase[9].

KLRG1⁺ cells have been used to differentiate central/memory and effector/memory cells based on expression of the CCR7 chemokine receptor. KLRG1⁺ CCR7⁺ cells are considered to be central/memory cells; KLRG1⁺ CCR7⁻ cells are considered to be effector/memory cells[11]. The ratio of effector/memory to central/memory KLRG1⁺ cells in the present study was ~3-fold greater regardless of the type of animal (Table 1). Thus, the lamina propria consists of a population of effector/memory cells, which increase in numbers in mice with chronic small intestinal inflammation due to an absence of Roquin-mediated control.

Chronic systemic inflammation is present in $Rc3h1^{gt/gt}$ and $Rc3h1^{gt/gt} \rightarrow$ NL chimeras. Chronic inflammatory responses also were evident in extra-intestinal tissues, most notably in the liver and spleen and to a lesser extent in the kidney and lung of $Rc3h1^{gt/gt}$ and $Rc3h1^{gt/gt} \rightarrow$ NL chimeras (Fig. 5, rows a and b, respectively), but was absent in the liver, spleen, kidney, and lung of NL → NL chimeras (Fig. 5, row c). Liver pathology consisted of intense mononuclear leukocytic infiltrate around the central vein and portal tract. The average liver pathology score of $Rc3h1^{gt/gt}$ and $Rc3h1^{gt/gt} \rightarrow$ NL chimeras is shown in Fig. 5d,

which indicates that there was more severe liver pathology in $Rc3h1^{gt/gt}$ mice compared to $Rc3h1^{gt/gt} \rightarrow$ NL chimeras.

$Rc3h1^{gt/gt}$ and $Rc3h1^{gt/gt} \rightarrow$ NL chimeras had chronic nephritis characterized by perivascular and interstitial mononuclear inflammatory infiltrate (Fig. 5, rows a and b, respectively). Necrotic hepatocytes associated with lymphocytic infiltrates were seen within the lobules without piece-meal necrosis. Lung tissue sections revealed lymphocytic pneumonitis characterized by perivascular and interstitial lymphocytic infiltrate with focal areas of interstitial fibrosis (Fig. 5, rows a and b, respectively). Splenic follicular hyperplasia, an immunopathological feature of $Rc3h1^{san/san}$ mice, was evident in $Rc3h1^{gt/gt}$ and $Rc3h1^{gt/gt} \rightarrow$ NL chimeras (Fig. 5, rows a and b, respectively). Although overall more $Rc3h1^{gt/gt}$ mice had inflammation in the liver, kidney, spleen, and lung than $Rc3h1^{gt/gt} \rightarrow$ NL chimeras, that difference was not statistically significant (Fig. 5e). In contrast, slightly more $Rc3h1^{gt/gt} \rightarrow$ NL chimeras had inflammation in the ileum compared to $Rc3h1^{gt/gt}$ mice, although this also was not statistically significant (Fig. 5e).

Caspase 3, a downstream effector caspase, plays a central role mediating apoptosis in a wide variety of cells. Hence, immunodetection of activated (cleaved) caspase 3 is frequently used to identify apoptosis in situ in tissue sections. Areas of cleaved caspase-3 positive hepatocytes were noted within the lobules and around the central veins and portal tract in the liver of $Rc3h1^{gt/gt}$ and $Rc3h1^{gt/gt} \rightarrow$ NL chimeras, but not NL → NL chimeras (Fig. 6a). This was the predominant area of chronic inflammatory cells infiltrate in liver sections (Fig. 5, liver panels a and b). These findings indicate that immune effector cells trigger apoptosis in adjacent hepatocytes.

Based on the above findings that $Rc3h1^{gt/gt}$ and $Rc3h1^{gt/gt} \rightarrow$ NL chimeras developed spontaneous perivascular and peribronchiolar lymphoid lung hyperplasia, whereas the lungs of NL → NL chimeras
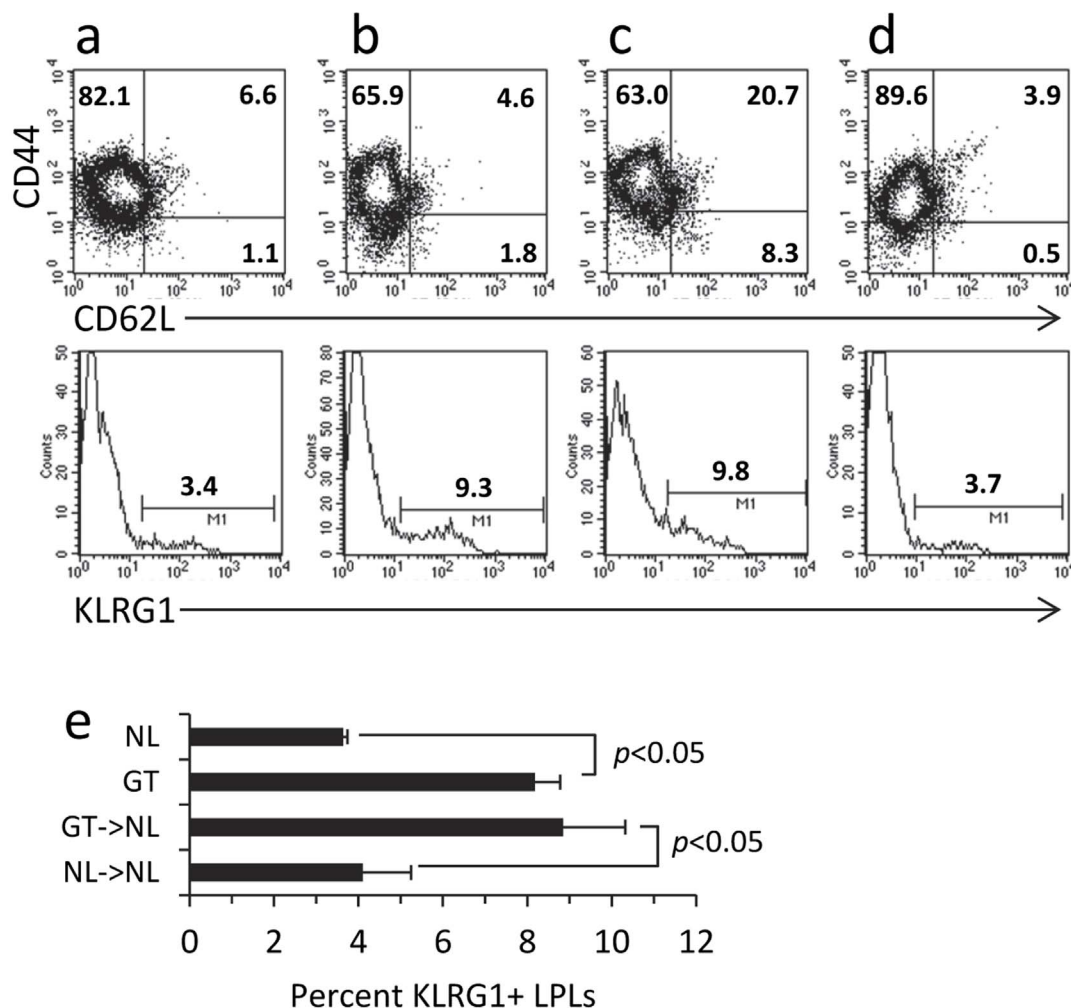
3

Figure 3 | CD44, CD62L, KLRG1 expression on LPLs from (a) NL mice, (b) *Rc3h1^gt/gt* mice (c) *Rc3h1^gt/gt* → NL chimeras, and (d) NL → NL chimeras. Determination of KLRG1 expression was done by gating onto the CD44^hi CD62L^lo population. (e) There were proportionally greater numbers of LPLs from *Rc3h1^gt/gt* mice and *Rc3h1^gt/gt* → NL chimeras expressing KLRG1 compared to their respective controls ($p < 0.05$). Mean values ± SEM of 2–3 samples per group.

had minimal inflammation, we analyzed the immunophenotypes of the pulmonary infiltrating cells by staining for the presence of CD3^{+} T cells and CD20^{+} B cells. Perivascular and peribronchiolar hyperplastic lymphoid cells in *Rc3h1^gt/gt* and *Rc3h1^gt/gt* → NL chimeras were composed predominantly of T cells (~60%) and B cells (~40%) (Fig. 6, panels b and c). In contrast, peribronchiolar and lobular inflammatory cells in NL → NL chimeras were mostly T cells (>90%) with a very few B-cells (<5%) (Fig. 6, panel c). These findings indicate that the lymphocytic infiltrate in the lungs of *Rc3h1^gt/gt* and *Rc3h1^gt/gt* → NL chimeras consist of lymphoid hyperplasia rather than lymphoma or prelymphoma neoplasia.

Collectively, these findings demonstrate that mice generated from BM of animals with targeted disruption of the *Rc3h1* gene develop extensive inflammation similar to that of *Rc3h1^san/san* and *Rc3h1^gt/gt* mice[7]. Because, the *Rc3h1* gene was unaltered in non-hematopoietic cells of *Rc3h1^gt/gt* → NL chimeras, the pathology which ensued in *Rc3h1^gt/gt* mice was attributable to the inflammatory response generated from cells of the immune system.

Oral infection of *Rc3h1^gt/gt* → NL chimeras with *L. monocytogenes* results in more liver pathology and greater numbers of bacteria in the Peyer's patches. We were interested in determining the extent to which the host response to an infectious agent, in this case *L. monocytogenes*, would differ in *Rc3h1^gt/gt* → NL chimeras and NL → NL chimeras. Groups of each type of animal were infected with bacteria[12] as described in the Methods. *Rc3h1^gt/gt* → NL chimeras had increased numbers of *L. monocytogenes* in Peyer's patches at day 2 post-infection (Fig. 7a), and greater liver pathology at day 4 post-infection (Fig. 7b), indicating that mice with ablated *Rc3h1* gene had a compromised response to oral *L. monocytogenes* infection.

Discussion

There is rapidly growing interest in Roquin due to its role in regulating the immune response and curtailing autoimmune pathology. Our recent studies were the first to examine the intestinal inflammatory response in *Rc3h1^san/san* mice, which have a mutation in the Roquin protein, and in *Rc3h1^gt/gt* mice, which have a disruption of the *Rc3h1* gene[7]. Both types of animals developed small intestinal inflammation in the ileum as well as in the duodenum and jejunum, though not in the colon[7]. The targeted feature of the inflammatory response to the small intestine in Roquin-mutant and Roquin-deficient mice is of particular significance given the lack of available animal models of Crohn's disease in the small intestine. Small intestine inflammation develops in TNF^ΔARE mice due to high levels of TNF expression[13,14], and in some mouse strains following parasitic infection[15]. Additionally, SAMP1/Yit mice spontaneously develop ileitis by 20–30 weeks of age[16,17]. Those animals are limited for studies into the underlying molecular basis of disease, however, because the genetic defect
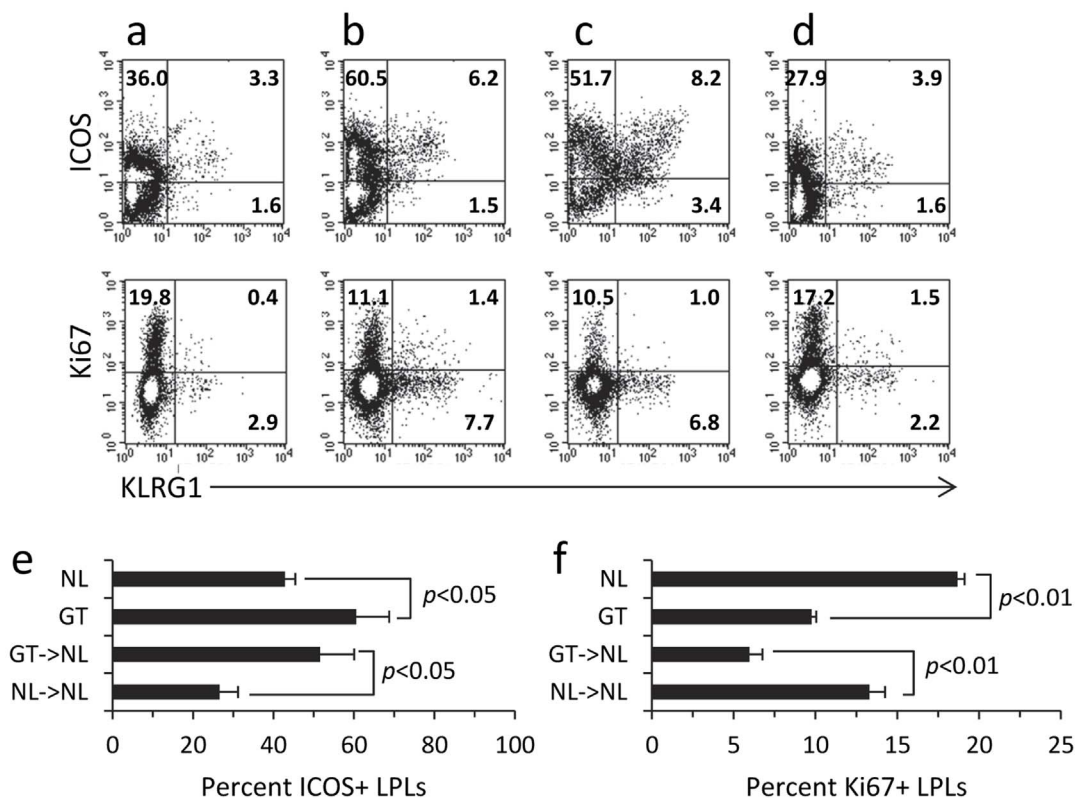
Figure 4 | KLRG1$^+$ cells in (a) NL mice, (b) $Rc3h1^{gt/gt}$ mice (c) $Rc3h1^{gt/gt} \rightarrow$ NL chimeras, and (d) NL $\rightarrow$ NL chimeras are predominantly ICOS$^+$ (top panel), and are Ki67$^-$ cells, indicating that they are activated non-proliferating cells. (e) ICOS is expressed on proportionally more LPLs from $Rc3h1^{gt/gt}$ mice and $Rc3h1^{gt/gt} \rightarrow$ NL chimeras compared to their respective controls ($p < 0.05$); mean values $\pm$ SEM of 2–3 samples per group. (f) LPLs from $Rc3h1^{gt/gt}$ mice and $Rc3h1^{gt/gt} \rightarrow$ NL chimeras have proportionally fewer Ki67$^+$ proliferating cells compared to their respective controls ($p < 0.01$). Mean values $\pm$ SEM of 2–3 samples per group.

has not been sufficiently characterized despite some progress in that area[18]. By contrast, the $Rc3h1$ gene and its paralog, $Rc3h2$, are well defined. The full gene and protein sequences are available and the chromosomal locations are known. The miR-223 microRNA has been shown to repress $Rc3h1$ gene expression[19], thereby providing additional information into the regulatory elements that control Roquin. Thus, the Roquin experimental system is ideal for studies into the molecular basis of autoimmunity in the gut and elsewhere.

The mode of action whereby Roquin represses inflammation in the intestine may involve suppression of IL-17 synthesis. Studies in our laboratory previously demonstrated an opposing relationship between Roquin expression and IL-17 production in the intestine[19]. We also observed that enforced expression of Roquin in IL-17-producing EL4 cells results in repressed IL-17 output (unpublished). This was confirmed in the present study by the experiments showing an increase in IL-17, IFNγ, and TNFα synthesis in $Rc3h1^{gt/gt} \rightarrow$ NL chimeras. Hence, it appears that one of the mechanisms whereby Roquin curbs the inflammatory response in the intestinal mucosa is via control of proinflammatory cytokine production.

There were notable differences in the degree of immunopathology in the $Rc3h1^{gt/gt}$ mice made in our laboratory and mice with a disrupted $Rc3h1$ gene produced by others. In an initial study, mice with $Rc3h1$ gene ablation failed to develop autoimmunity despite high post-birth mortality[8]. In two subsequent studies, a $Rc3h1^{san/san}$ -like phenotype was present in mice with combined disruption of $Rc3h1$ and its paralog, $Rc3h2$[20,21]. Although the basis for the differences between those findings and ours remain unclear, $Rc3h1^{gt/gt}$ mice made in our laboratory consistently and reliably developed small intestinal inflammation, particularly in the ileum where 92.3% of $Rc3h1^{gt/gt}$ mice and $Rc3h1^{gt/gt} \rightarrow$ NL chimeras developed an inflammatory response. Because $Rc3h1^{gt/gt}$ mice made in our laboratory were generated by a random insertion of a gene-trap into the murine genome, the likelihood of simultaneous insertion into both the $Rc3h1$ and $Rc3h2$ genes was extremely remote. We therefore conclude, based on the studies here and our previous work[7], that ablation of only the $Rc3h1$ gene is by itself sufficient to render an autoimmune phenotype in mice. It should be noted, however, that Roquin-1 and Roquin-2 expression were reported to be variable in mice throughout various immunological compartments[21]. If, in fact, Roquin-2 is capable of compensating for and mollifying the autoimmune response caused by deregulation of Roquin-1, as suggested[20,21], tissues with low Roquin-2 synthesis would be particularly prone to autoimmunity while other tissues may be spared. As yet unknown tissue-specific cofactors also may be necessary for optimal Roquin-mediated repression[5,21].

KLRG1 is a type 2 integral membrane protein of the C-type lectin family that has been linked to a number of function-related activities. In mice, KLRG1 is expressed on NK cells and also defines a set of T cells that have effector activity but lack antigen-induced proliferation[9,11]. E-cadherin, the KLRG1 ligand, is expressed on epithelial cells

Table 1 | Ratio of KLRG1$^+$ CCR7$^-$ Effector/Memory : KLRG1$^+$ CCR7$^+$ Central/Memory LPLs

NL	$Rc3h1^{gt/gt}$	$Rc3h1^{gt/gt} \rightarrow$ NL	NL $\rightarrow$ NL
3.30 ± 1.32^{a,b}	3.43 ± 1.5^{a,b}	3.93 ± 0.66^{a,b}	3.15 ± 0.22^{a,b}

^{a}Mean values ± SEM.
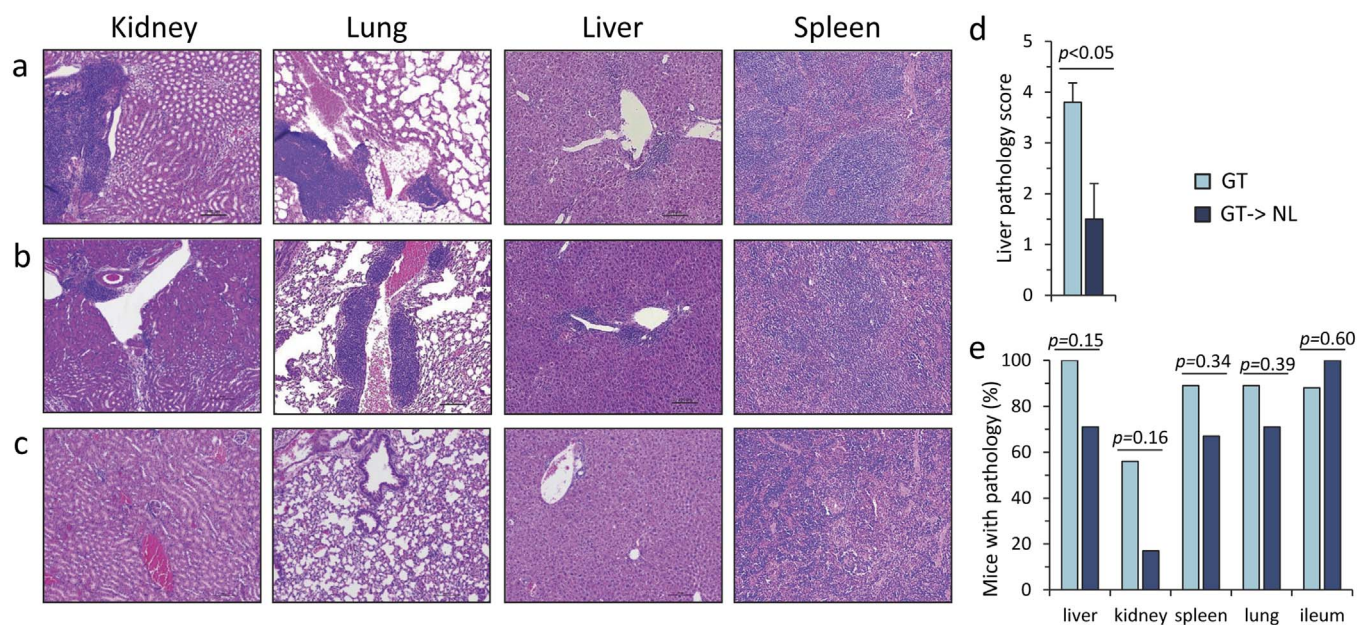^{b}$p > 0.05$ compared to other animal groups.

Figure 5 | Histopathological analysis of tissue sections from the kidney, lung, liver, and spleen from (a) $Rc3h1^{gt/gt}$ mice, (b) $Rc3h1^{gt/gt} \to$ NL chimeras, and (c) NL $\to$ NL chimeras. Inflammation was most common in the liver of $Rc3h1^{gt/gt}$ and $Rc3h1^{gt/gt} \to$ NL chimeras, and was less common in the kidney, lung, and spleen. Inflammation was absent in the kidney, lung, and liver of NL $\to$ NL chimeras. Micrographs are 100 $\times$ original magnification; scale bars are 100 μm. (d) Mean liver scores $\pm$ SEM of 10 $Rc3h1^{gt/gt}$ mice and 8 $Rc3h1^{gt/gt} \to$ NL chimeras. * $p < 0.05$ comparing $Rc3h1^{gt/gt}$ mice and $Rc3h1^{gt/gt}$ $\to$ NL chimeras. (e) Percent of mice with inflammation in the liver, kidney, spleen, lung, and ileum of $Rc3h1^{gt/gt}$ mice compared to $Rc3h1^{gt/gt} \to$ NL chimeras.

and on some classical antigen presenting cells, in particular Langerhans cells[22]. E-cadherin is expressed at high levels on the intestinal epithelium[23], thus providing continual expression of the KLRG1 ligand. Blockade of E-cadherin has been shown to enhance T cell proliferation. It was recently demonstrated that treatment of mice with an agonistic antibody to the 4-1BB T cell activation marker induced a novel population of KLRG1^{+} effector cells to infiltrate melanoma tumors[24]. The finding reported here that proportionally
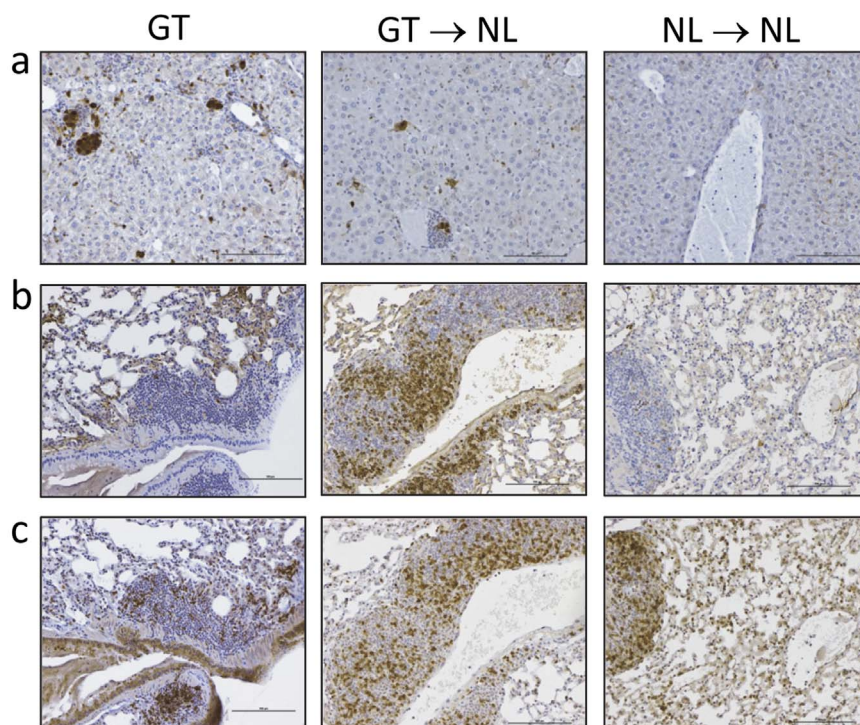

Figure 6 | (a) Caspase 3 expression in the liver of $Rc3h1^{gt/gt}$ mice (GT), $Rc3h1^{gt/gt} \to$ NL chimeras (GT $\to$ NL), and NL $\to$ NL chimeras, showing increased caspase staining in mice with ablated $Rc3h1$. Lung tissues in the three groups of mice stained for the presence of (b) CD20^{+} B cells and (c) CD3^{+} T cells. Note the abundance of B cells in mice with ablated Rc3h1 compared to lung tissue from control mice. Micrographs are 100 $\times$ original magnification; scale bars are 100 μm.
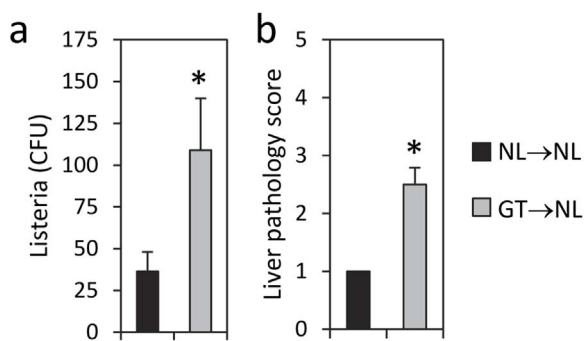
Figure 7 | Effect of oral infection in Rc3h1$^{gt/gt}$ → NL chimeras. Rc3h1$^{gt/gt}$ → NL chimeras and NL → NL chimeras were infected orally with *L. monocytogenes* as described in the Methods. Rc3h1$^{gt/gt}$ → NL chimeras had (a) more bacteria in the Peyer's patches, and (b) more liver pathology than NL → NL chimeras. *$p < 0.05$. Mean values ± SEM of 3 mice per group.

more CD44^{hi} CD62L^{lo} KLRG1$^+$ cells infiltrate the lamina propria of Rc3h1$^{gt/gt}$ mice and Rc3h1$^{gt/gt}$ → NL chimeras than normal mice is consistent with an increase in effector T cells and provides a logical explanation for the basis of small intestinal inflammation in those animals. This is further reinforced by our observation of increased ICOS expression on KLRG1$^+$ cells. That most KLRG1$^+$ cells in Rc3h1$^{gt/gt}$ mice and Rc3h1$^{gt/gt}$ → NL chimeras as well as their normal animal counterparts were Ki67$^-$ and thus non-proliferating cells also is consistent with the KLRG1 phenotype. Aligned with that, KLRG1$^+$ cells were predominantly effector/memory cells based on the lack of CCR7 expression[11].

Rc3h1$^{gt/gt}$ → NL chimeras were more susceptible to oral infection with *L. monocytogenes* than NL → NL chimeras as determined by the presence of liver pathology and the numbers of bacteria in the Peyer's patches, suggesting that although Rc3h1$^{gt/gt}$ → NL chimeras developed a strong intestinal inflammatory response, they were less capable of mounting an antigen-reactive response. The basis for this remains unclear; however, it could reflect the concomitant generation of suppressive effector cells. Additional studies will be needed to address this.

Finally, it is worth noting that the full functional role of Roquin remains to be elucidated. It is possible, for example, that the evolutionary adaptation of Roquin is primarily geared toward activating the immune system in a beneficial manner rather than suppressing it. This could occur by repressing Roquin expression during the early phase of an immune response, thus leading to increased expression of ICOS and OX40, two key molecules used during T cell activation. In that context, it was recently demonstrated that although enforced expression of Roquin resulted in repressed ICOS expression, CD28 expression and CD28-mediated immunity were concomitantly augmented[25]. Clearly, autoimmunity could develop if sufficient stimuli exist for sustained Roquin suppression. The studies reported here demonstrate that Roquin has the capacity to control chronic inflammation in the intestine and elsewhere. Additional experimental work using mice with defective Roquin expression will be useful for addressing this Roquin paradox.

Methods

Rc3h1$^{gt/gt}$ mice and BM radiation chimeras. The method used to generate Rc3h1$^{gt/gt}$ mice has been previously described[7]. Animals were bred to homozygosity for more than nine generations onto a C57BL/6 background. Hematopoietic radiation chimeras were made by injecting 5–10 × 10^6 BM cells from Rc3h1$^{gt/gt}$ mice into NL syngeneic gender-matched mice by retro-orbital[26] injection within 4 hrs of 900 cGy total body irradiation (Rc3h1$^{gt/gt}$ → NL chimeras). Control radiation chimeras were generated using NL C57BL/6 BM injected into syngeneic gender-matched mice (NL → NL chimeras). C57BL/6 mice were purchased from Harlan (Indianapolis, IN). Mice were used in accord with the University of Texas Health Science Center at Houston Institutional Animal Welfare Committee. The use of animals for the experiments conducted in this study was approved by permit No. HSC-AWC-12-039

of the University of Texas Health Science Center at Houston Animal Welfare Committee.

Histopathological analyses. Representative H&E stained tissue sections from the duodenum, jejunum, ileum, cecum, ascending colon, transverse colon, descending colon, liver, kidney, lung, and spleen were examined by a board-certified pathologist blinded to the study groups. Intestinal inflammation and associated villi injury for each section was graded by summing up the scores for inflammation and villi and crypt injury as described previously[7]. The degree of inflammation and hepatocyte necrosis in liver sections was graded using a modified scoring system as described previously[7]. Tissue sections of lung and kidney were examined for inflammation, tissue injury, and fibrosis.

Cell isolation and staining. Intestinal lamina propria leukocytes (LPLs) were isolated and stained as previously reported[7]. Antibodies used were: PE-anti-CD8α (53-6.7); PE-anti-CD278 (ICOS) (7E.17G9); FITC-anti-CD44 (IM7); PE-anti-CD44 (SolA15); AlexaFluor 647- anti-Ki67 (SolA15); APC-anti-KLRG1 (2F1); APC- and FITC-anti-IL-17A (eBiol17B7); FITC-anti-IFNγ (XMG1.2); FITC-anti-TNFα (MP6-XT22); APC-anti-IL-10 (JES5-16E3); FITC rat IgG isotype control (eBRG1); biotin rat IgG isotype control; PE rat IgG2a isotype control (eBR2a); streptavidin APC (eBioscience, San Diego, CA, all reagents); PE-anti-CD62L (MEL-17) (Pharmingen, San Diego, CA); anti-CD20/MS4A1 (L26); anti-CD3/TCRE (SP7) (Thermo Fisher Scientific; Rockford, IL); cleaved caspase-3[27] (Asp175) (Cell Signaling Technology; Danvers, MA). Intracellular cytokine stainings were done as previously reported by our laboratory[28]. Liver and lung stainings for detection of caspase activity and for CD20 and CD3 were done using representative formalin fixed paraffin embedded tissue sections after deparaffinization and rehydration, and subjected to antigen retrieval by heating in target antigen retrieval solution (ANTIGEN*DECLOAKER*^{TM}, Biocare Medical, Concord, CA) according to the manufacturer's instructions. Endogenous peroxidase activity was quenched by incubating the tissue section with 3% H$_2$O$_2$ in methanol for ten minutes. Non-specific binding sites were blocked by incubating the tumor sections in BACKGROUND TERMINATOR (Biocare Medical) solution for ten minutes. Immunoreactivity of mouse monoclonal antibodies against mouse tissue (CD20) was detected using the Vector® M.O.M.^{TM} Kit with ImPRESS^{TM} peroxidase polymer (Vector Laboratories, Inc, Burlingame, CA) according to the protocol provided with the kit. A Vectastatin Elite ABC kit was used for detecting immunoreactivity of antibodies. Immunoperoxidase reactive sites in tissue sections were visualized using diaminobenzidine tetrachloride as chromogenic substrate. The tissue sections were counterstained with hematoxylin. Non-immune mouse or rabbit serum was used for negative control staining.

***L. monocytogenes* infection.** *L. monocytogenes* serotype 4b was purchased from American Type Culture Collection, Manassas, VA. Bacteria were grown in brain heart infusion broth (Fischer). Stock titers were determined to be 1.79 × 10^{14} CFU/ml based on serial dilutions onto brain heart infusion agar plates. Rc3h1$^{gt/gt}$ → NL chimeras and NL → NL chimeras were inoculated by oral gavage with 200 μl undiluted stock. 2 days post-infection, groups of mice were euthanized, and Peyer's patches were recovered from the small intestine. Tissues were minced and separated using a Dounce homogenizer. A second group of mice was euthanized on day 4 post-infection; liver tissues were fixed and prepared for histopathological analyses.

Statistical analyses. Student's t-test was used for determination of statistical significance with the exception of comparisons of the percent of mice with pathology, which used a Fisher exact probability test.

1. Ciechanover, A. The ubiquitin-proteasome pathway: on protein death and cell life. *Embo J* **17**, 7151–7160 (1998).
2. Lin, A. E. & Mak, T. W. The role of E3 ligases in autoimmunity and the regulation of autoreactive T cells. *Curr Opin Immunol* **19**, 665–673 (2007).
3. Vinuesa, C. G. *et al.* A RING-type ubiquitin ligase family member required to repress follicular helper T cells and autoimmunity. *Nature* **435**, 452–458 (2005).
4. Yu, D. *et al.* Roquin represses autoimmunity by limiting inducible T-cell co-stimulator messenger RNA. *Nature* **450**, 299–303 (2007).
5. Heissmeyer, V. & Vogel, K. U. Molecular control of Tfh-cell differentiation by Roquin family proteins. *Immunol Rev* **253**, 273–289 (2013).
6. Leppek, K. *et al.* Roquin promotes constitutive mRNA decay via a conserved class of stem-loop recognition motifs. *Cell* **153**, 869–881 (2013).
7. Schaefer, J. S., Montufar-Solis, D., Nakra, N., Vigneswaran, N. & Klein, J. R. Small intestine inflammation in roquin-mutant and roquin-deficient mice. *PloS one* **8**, e56436 (2013).
8. Bertossi, A. *et al.* Loss of Roquin induces early death and immune deregulation but not autoimmunity. *J Exp Med* **208**, 1749–1756 (2011).
9. Voehringer, D. *et al.* Viral infections induce abundant numbers of senescent CD8 T cells. *J Immunol* **167** (2001).
10. Scholzen, T. & Gerdes, J. The Ki-67 protein: from the known and the unknown. *J Cell Physiol* **182**, 311–322 (2000).
11. Voehringer, D., Koschella, M. & Pircher, H. Lack of proliferative capacity of human effector and memory T cells expressing killer cell lectinlike receptor G1 (KLRG1). *Blood* **100**, 3698–3702 (2002).
12. MacDonald, T. T. & Carter, P. B. Cell-mediated immunity to intestinal infection. *Infect Immun* **28** (1980).

13. Kontoyiannis, D., Pasparakis, M., Pizarro, T. T., Cominelli, F. & Kollias, G. Impaired on/off regulation of TNF biosynthesis in mice lacking TNF AU-rich elements: implications for joint and gut-associated immunopathologies. *Immunity* **10**, 387–398 (1999).

14. Armaka, M. *et al.* Mesenchymal cell targeting by TNF as a common pathogenic principle in chronic inflammatory joint and intestinal diseases. *J Exp Med* **205**, 331–337 (2008).

15. Egan, C. E., Cohen, S. B. & Denkers, E. Y. Insights into inflammatory bowel disease using Toxoplasma gondii as an infectious trigger. *Immunol Cell Biol* **90**, 668–675 (2012).

16. Rivera-Nieves, J. *et al.* Emergence of perianal fistulizing disease in the SAMP1/YitFc mouse, a spontaneous model of chronic ileitis. *Gastroent* **124**, 972–982 (2003).

17. Matsumoto, S. *et al.* Inflammatory bowel disease-like enteritis and caecitis in a senescence accelerated mouse P1/Yit strain. *Gut* **43**, 71–78 (1998).

18. Kozaiwa, K. *et al.* Identification of a quantitative trait locus for ileitis in a spontaneous mouse model of Crohn's disease: SAMP1/YitFc. *Gastroent* **125**, 477–490 (2003).

19. Schaefer, J. S., Montufar-Solis, D., Vigneswaran, N. & Klein, J. R. Selective upregulation of microRNA expression in peripheral blood leukocytes in IL-10-/- mice precedes expression in the colon. *J Immunol* **187**, 5834–5841 (2011).

20. Pratama, A. *et al.* Roquin-2 shares functions with its paralog Roquin-1 in the repression of mRNAs controlling T follicular helper cells and systemic inflammation. *Immunity* **38**, 669–680 (2013).

21. Vogel, K. U. *et al.* Roquin paralogs 1 and 2 redundantly repress the Icos and Ox40 costimulator mRNAs and control follicular helper T cell differentiation. *Immunity* **38**, 655–668 (2013).

22. Henson, S. M. & Akbar, A. N. KLRG1--more than a marker for T cell senescence. *Age* **31**, 285–291 (2009).

23. Bagriacik, E. U., Tang, M., Wang, H. C. & Klein, J. R. CD43 potentiates CD3-induced proliferation of murine intestinal intraepithelial lymphocytes. *Immunol Cell Biol* **79**, 303–307 (2001).

24. Curran, M. A. *et al.* Systemic 4-1BB activation induces a novel T cell phenotype driven by high expression of Eomesodermin. *J Exp Med* **210**, 743–755 (2013).

25. Kim, H. J. *et al.* The role of Roquin overexpression in the modulation of signaling during in vitro and ex vivo T-cell activation. *Biochem Biophys Res Commun* **417**, 280–286 (2012).

26. Yardeni, T., Eckhaus, M., Morris, H. D., Huizing, M. & Hoogstraten-Miller, S. Retro-orbital injections in mice. *Lab Anim* **40**, 155–160 (2011).

27. Gown, A. M. & Willingham, M. C. Improved detection of apoptotic cells in archival paraffin sections: immunohistochemistry using antibodies to cleaved caspase 3. *J Histochem Cytochem* **50**, 449–454 (2002).

28. Schaefer, J. S., Montufar-Solis, D., Vigneswaran, N. & Klein, J. R. ICOS promotes IL-17 synthesis in colonic intraepithelial lymphocytes in IL-10-/- mice. *J Leuk Biol* **87**, 301–308 (2010).

Author contributions

J.R.K. conceived and designed the experiments, D.M.-S., N.V., N.N. and J.S.S. performed the experiments. J.R.K., N.V., D.M.-S., J.S.S. and N.N. analyzed the data. J.R.K., N.V. and J.S.S. wrote the paper.

Additional information

How to cite this article: Montufar-Solis, D., Vigneswaran, N., Nakra, N., Schaefer, J.S. & Klein, J.R. Hematopoietic not systemic impairment of Roquin expression accounts for intestinal inflammation in Roquin-deficient mice. *Sci. Rep.* **4**, 4920; DOI:10.1038/srep04920 (2014).